Applied Geochemistry 71 (2016) 48–62

Contents lists available at ScienceDirect

Applied Geochemistry

journal homepage: www.elsevier.com/locate/apgeochem

Groundwater recharge and salinization in the arid coastal plain aquifer of the Wadi Watir delta, Sinai, Egypt

Mustafa A. Eissa [a, c, d], James M. Thomas [b, *], Greg Pohll [b], Orfan Shouakar-Stash [c, d, e], Ronald L. Hershey [b], Maher Dawoud [f]

[a] Desert Research Center, Hydrogeochemistry Dept., Cairo, Egypt
[b] Desert Research Institute, Division of Hydrologic Sciences, Reno, NV, USA
[c] Isotope Tracer Technologies INC, Waterloo, Ontario, Canada
[d] University of Guelph, G 360 Group, Center of Applied Groundwater Research, Guelph, Ontario, Canada
[e] University of Waterloo, Department of Earth Sciences, Waterloo, Ontario, Canada
[f] Menoufiya University, Geology Department, Menoufiya, Egypt

A R T I C L E I N F O

Article history:
Received 26 October 2015
Received in revised form
24 May 2016
Accepted 27 May 2016
Available online 28 May 2016

Keywords:
Salinization
Groundwater sustainability
Groundwater modeling
Seawater intrusion
Water chemistry
Isotopes
Wadi Watir Egypt

A B S T R A C T

The Quaternary coastal plain aquifer down gradient of the Wadi Watir catchment is the main source of potable groundwater in the arid region of south Sinai, Egypt. The scarcity of rainfall over the last decade, combined with high groundwater pumping rates, have resulted in water-quality degradation in the main well field and in wells along the coast. Understanding the sources of groundwater salinization and amount of average annual recharge is critical for developing sustainable groundwater management strategies for the long-term prevention of groundwater quality deterioration. A combination of geochemistry, conservative ions (Cl and Br), and isotopic tracers ($^{87/86}$Sr, δ^{81}Br, δ^{37}Cl), in conjunction with groundwater modeling, is an effective method to assess and manage groundwater resources in the Wadi Watir delta aquifers. High groundwater salinity, including high Cl and Br concentrations, is recorded inland in the deep drilled wells located in the main well field and in wells along the coast. The range of Cl/Br ratios for shallow and deep groundwaters in the delta (~50–97) fall between the end member values of the recharge water that comes from the up gradient watershed, and evaporated seawater of marine origin, which is significantly different than the ratio in modern seawater (228). The $^{87/86}$Sr and δ^{81}Br isotopic values were higher in the recharge water ($0.70,723 < {}^{87/86}Sr < 0.70,894$, $+0.94 < \delta^{81}Br < +1.28‰$), and lower in the deep groundwater ($0.70,698 < {}^{87/86}Sr < 0.70,705$, $+0.22‰ < \delta^{81}Br < +0.41‰$). The δ^{37}Cl isotopic values were lower in the recharge water ($-0.48 < \delta^{37}Cl < -0.06‰$) and higher in the deep groundwater ($-0.01 < \delta^{37}Cl < +0.22‰$). The isotopic values of strontium, chloride, and bromide in groundwater from the Wadi Watir delta aquifers indicate that the main groundwater recharge source comes from the up gradient catchment along the main stream channel entering the delta. The solute-weighted mass balance mixing models show that groundwater in the main well field contains 4–10% deep saline groundwater, and groundwater in some wells along the coast contain 2–6% seawater and 18–29% deep saline groundwater.

A three-dimensional, variable-density, flow-and-transport SEAWAT model was developed using groundwater isotopes (^{87}Sr/^{86}Sr, δ^{37}Cl and δ^{81}Br) and calibrated using historical records of groundwater level and salinity. δ^{18}O was used to normalize the evaporative effect on shallow groundwater salinity for model calibration. The model shows how groundwater salinity and hydrologic data can be used in SEAWAT to understand recharge mechanisms, estimate groundwater recharge rates, and simulate the upwelling of deep saline groundwater and seawater intrusion. The model indicates that most of the groundwater recharge occurs near the outlet of the main channel. Average annual recharge to delta alluvial aquifers for 1982 to 2009 is estimated to be 2.16×10^6 m^3/yr. The main factors that control groundwater salinity are overpumping and recharge availability.

* Corresponding author.
E-mail address: Jim.Thomas@dri.edu (J.M. Thomas).

http://dx.doi.org/10.1016/j.apgeochem.2016.05.017

1. Introduction

Alluvial aquifers in arid to semiarid coastal regions worldwide supply freshwater, such as the coastal plain aquifers in the Nile Delta (Sefelnasr and Sherif, 2014) along the northwestern coast of Egypt (Eissa et al., 2015a;b), the Korba plain in Tunisia (Salma et al., 2010), the Eastern Batinah region in northern Oman (Weyhenmeyer, 2002), and along the Arabian Gulf in northern United Arab Emirates (Alsharhan et al., 2001). In the Wadi Watir delta in Sinai, Egypt, as in many arid coastal regions of the world, potable water is limited to a shallow alluvial aquifer that provides the main potable water supply for Nuweiba Harbor located on the coast of the Gulf of Aqaba (Fig. 1). In this aquifer, a thin lens of groundwater floats over a deep saline layer that is very sensitive to pumping induced stresses (El Kiki et al., 1992; El-Refaei, 1992; Eissa et al., 2010). The aquifer has a thickness of about 90 m and high porosity that exceeds 30% (Khalil, 2010). Excessive groundwater withdrawal, undertaken to meet increasing water demands, has resulted in a declining water table, groundwater salinization from an upwelling of deep saline groundwater beneath the delta aquifer (Ismail, 1998; El Sayed, 2006; Shalaby, 1997; Mabrouk and Nasr, 1997), and seawater intrusion at the coast (Abuelfadl, 2004; Abd El Hafez, 2001). The delta was filled with high-saline water during the Pleistocene epoch and its deep layers are composed of mainly clayey sand and clay intercalations that represent three sequential phases of regression and transgression of gulf water (Abbas et al., 2004; Mabrouk and Nasr, 1997). In the Gulf of Aqaba drainage system, recharge is limited throughout the dry season, and groundwater salinization becomes a severe problem (Himida, 1997; Eissa et al., 2010; Isawi et al., 2016). Therefore, understanding the groundwater recharge sources and the upwelling mechanism of deep saline groundwater are important for groundwater management, and necessary to ensure groundwater sustainability at local and regional scales.

In this study, groundwater chemistry and multiple isotopes ($^{87/86}$Sr, δ^{37}Cl, δ^{81}Br, and δ^{18}O), combined with groundwater modeling, were used to evaluate the water-rock interactions, the origin of groundwater recharge, seawater mixing, and the upwelling of deep saline groundwater in the delta. The isotopes used in this study have been used in previous studies to better understand the origin of deep groundwater salinization and improve the understanding of the hydrogeological system of the Canadian Shield, the Russian Siberian Platform, and deep groundwater from Vienne granitoids in France (Stotler et al., 2010; Shouakar-Stash et al., 2007; Negrel et al., 2002).

The variable density groundwater SEAWAT model is an efficient tool for understanding groundwater hydrodynamics, tracing the upwelling of deep saline water, quantifying seasonal variations in groundwater recharge, and evaluating seawater intrusion along coastal aquifers (Guo and Langevin, 2002). However, the assessment and accuracy of the model's output, including groundwater recharge and solute transport, mainly depend on the uncertainty of the input hydrologic parameters (Sibanda et al., 2009). Therefore, using environmental isotopes in conjunction with a numerical flow model could provide further insights into the hydrogeological model framework and model calibration. Several mathematical flow models have been used for the quantitative evaluation and formulation of isotopic data in a hydrological system (IAEA, 1993; Malosazewski et al., 1989). Isotope tracers have been used to provide further insights into the hydraulic properties of natural hydrogeologic systems in an Alpine catchment in Germany (Plumacher and Kinzelbach, 2000), and to calibrate regional groundwater flow models for carbonate-alluvial groundwater systems in southern Nevada in the United States (Kirk and Campana, 1990). Natural isotope (δ^{18}O and δ^{2}H) approach models have been used in combination with numerical models to evaluate groundwater recharge in an alluvial aquifer in the Nasunogahara area in central Japan (Liu et al., 2014).

In this study, isotopes were used to provide qualitative data for helping to understand the hydrogeological flow system, such as system boundaries, processes of replenishment, and the origins of groundwater recharge and salinization. Quantitative data were inferred, such as the mixing ratios of different water sources and the evaporation factor for shallow groundwater, from these isotopic data. δ^{18}O values were used to calculate the amount of groundwater evaporation, which was needed for estimating the normalized groundwater salinity needed for SEAWAT model calibration.

This study aimed to: (1) determine the primary source(s) of groundwater salinization in the main well field and gain a better understanding of the effect of deep saline groundwater, (2) develop a SEAWAT model framework based on the isotopic data and the dominant processes that affect groundwater in the Wadi Watir delta, (3) improve SEAWAT model calibration using groundwater level and normalized groundwater salinity data, and (4) estimate the seasonal groundwater recharge sources and rates in the alluvial coastal aquifer system using a tracer approach and numerical simulations.

2. Study area, geology, and hydrogeology

The Wadi Watir delta is located down gradient of the Wadi Watir watershed on the southeastern part of the Sinai Peninsula, Egypt, between longitude 34° 38′ and 34° 41′ E and latitude 28° 57′ and 29° 03′ N (Fig. 1). The Wadi Watir watershed is considered to be the most important watershed in this region because the city of Nuweiba, a tourist destination, and Nuweiba Harbor are on the coast of this delta. Ships sailing from Nuweiba Harbor connect Egypt, Saudi Arabia, and Jordan.

The Wadi Watir watershed is predominantly composed of Precambrian granitic, metamorphic, and volcanic rocks intruded by acidic to basic dykes (Said, 1962). The watershed formed as a part of the eastern tectonic rift of the Sinai, which is delineated by a series of shear faults that form structurally elongated downfaulted rift valleys (Eyal, 1973; Bartov et al., 1979a,b). The rift is mainly composed of Paleozoic clastic and carbonate rocks and is covered by recent Quaternary alluvial deposits (Issar and Gilad, 1982). The Wadi Watir delta is comprised of alluvial aquifers underlain by an impermeable Precambrian basement (Fig. 2).

Groundwater from El Shiekh Attia, the Main Channel, and Furtaga Springs (site $At_{1,2}$, Mc, and F_1; Figs. 1 and 2) are the main recharge sources of groundwater and are located up gradient of the alluvial aquifers of the delta (El Ghazawi, 1999; Eissa et al., 2013b). The primary potable water supply for the Wadi Watir delta is from a well field located adjacent to the mountain block where the Wadi Watir watershed drainage enters the delta (Fig. 1; sites 17–23). Well pumping began in 1982 and since that time, the pumping rate has varied depending on groundwater availability and recharge (El Ghazawi, 1999). The major source of recharge to the alluvial aquifers of the Wadi Watir delta is infiltration from infrequent, heavy rains and floods in the mountain block area of the Wadi Watir watershed (El-Refaei, 1992).

The delta alluvial deposits are mainly composed of Quaternary fine-to-coarse sands, gravels, and boulders that are often within a silty and clayey matrix. These deposits are primarily derived from carbonate and basement rocks (El-Shazly et al., 1974; Eyal et al., 1980; El Kiki et al., 1992). The Quaternary deposits of the Wadi Watir delta can be divided into five layers (Fig. 2b, modified from Abbas et al., (2004)). The two uppermost layers are generally <10 m thick, grouped as surface layers, and are comprised of heterogeneous alluvial deposits. The third layer is a sandy-clay layer that is

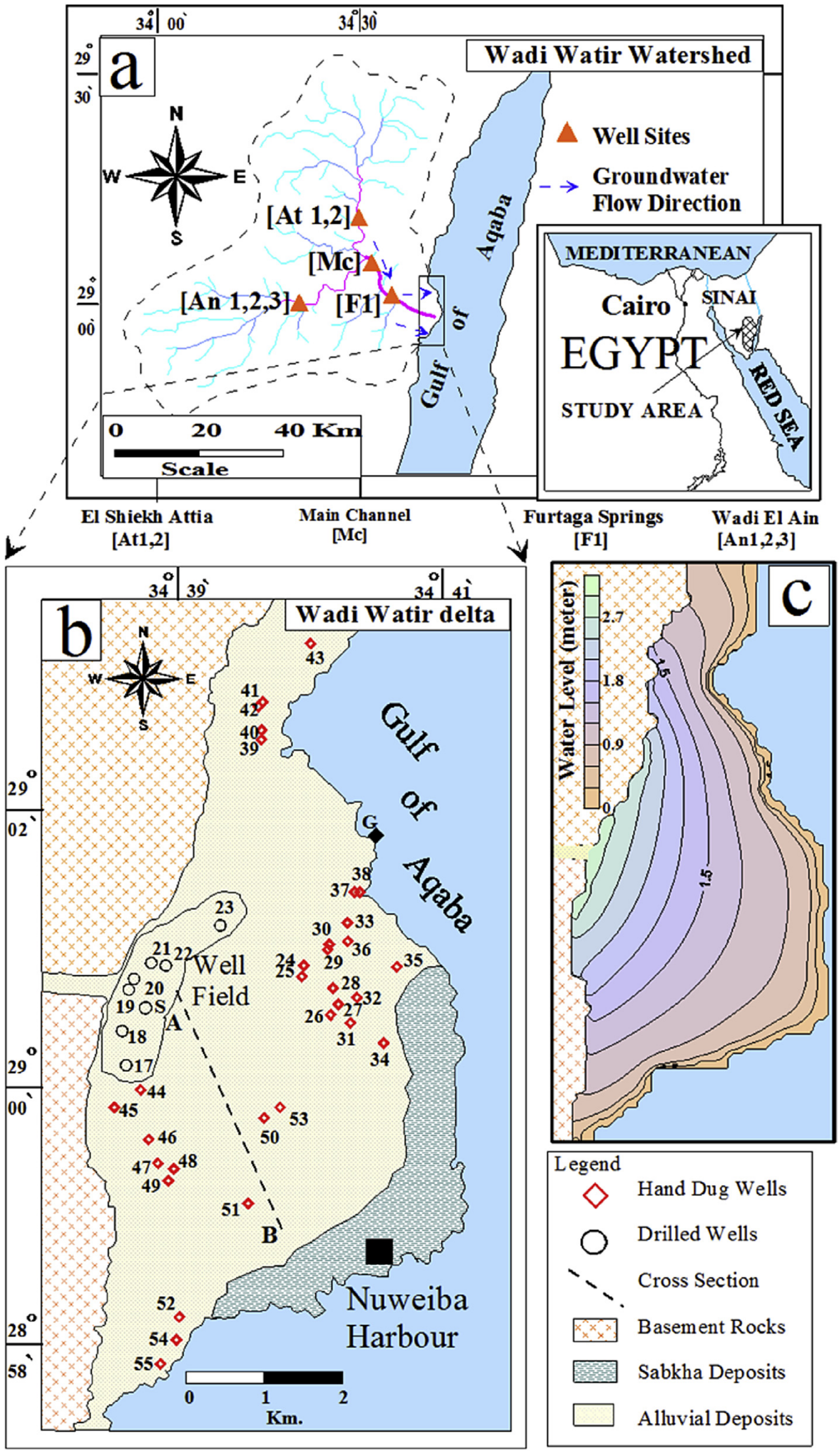

Fig. 1. a) Location map of the Wadi Watir watershed, Sinai Peninsula, Egypt. b) Location map of the Wadi Watir delta and groundwater wells. Dashed line A-B indicates location of cross section shown in Fig. 2 c) Water level map of Wadi Watir delta aquifers.

30–45 m thick. The fourth layer is alluvial clastic sand and gravel that is 20–40 m thick. The fifth layer is sand with interlayered clay that is 20–50 m thick. These five layers are underlain by bedrock that is mainly composed of very-low-permeability granitic rocks.

The Wadi Watir delta alluvial aquifers are unconfined water-table aquifers. The depth to water in these aquifers ranges from 2.3 to 40.8 m below land surface. Water levels in the Wadi Watir delta aquifers vary from <1 to approximately 2.3 m above sea level (Eissa

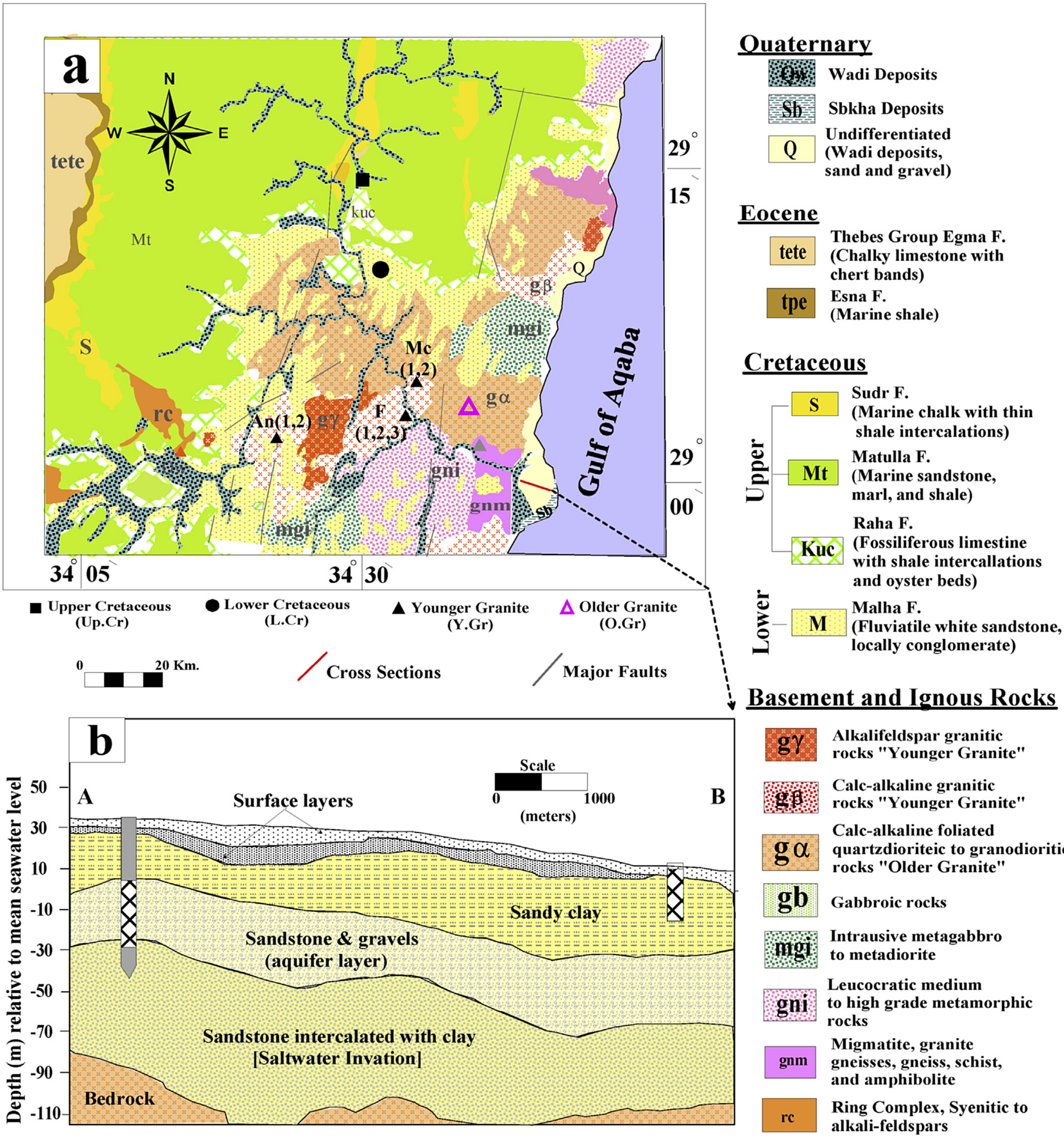

Fig. 2. a) Geological map of the Wadi Watir watershed and b) stratigraphic cross section of the Wadi Watir delta constructed from vertical electric sounding field data (modified from Abbas et al., (2004)). The location of the cross section is shown in Fig. 1 and is in a northwest-southeast direction across the delta (A–B).

et al., 2013a).

3. Methods

3.1. Field and laboratory methods

Thirty-nine water samples were collected from 32 hand-dug wells and seven drilled wells in March 2007. In September 2009, an additional six samples were collected from the well field area (Fig. 1 and SM 1). Rock samples representing different aquifers located in the watershed above the delta were collected from four different locations: the Wadi El Ain ($An_{1,2,3}$), Main Channel (Mc), Furtaga Springs ($F_{1,2,3}$), and El Shiekh Attia areas ($At_{1,2}$) (SM 1, Table 1; Figs. 1 and 2). The depth to water, total well depth, pH, and electrical conductivity (EC) were measured in the field. The EC was measured using a YSI model 35 conductivity meter. The pH was measured using a WTW model LF 538 pH meter. The EC and pH meters were calibrated daily. Water samples were filtered in the field using a 0.45 μm cellulose acetate filter and samples for major-ion and isotope analyses were collected in polyethylene bottles. Major-ion water chemistry analyses (SM 1) were conducted in Cairo, Egypt, at the Desert Research Center, Water Central Laboratory using the standard methods of Rainwater and Thatcher (1960) and Fishman and Friedman (1985). Chemical analyses for major ions were accepted only when the charge balance for the cations and anions was less than ±5%.

To determine the isotopic ratio signatures for different rocks within different aquifers located up gradient of the Wadi Watir delta, twenty rock samples were crushed and ground to a fine powder. A 1:1 vol ratio of water and rock was shaken for three weeks to obtain equilibrium. The samples were centrifuged and filtered through a 0.45 μm filter paper to obtain the water extract for each sample and isotopic signatures for $\delta^{37}Cl$, $\delta^{81}Br$, and $^{87}Sr/^{86}Sr$. The $\delta^{37}Cl$, $\delta^{81}Br$, and $^{87}Sr/^{86}Sr$ samples were analyzed at Isotope Tracer Technologies Inc. (IT^2), in Waterloo, Canada (Table 1). The method and procedures described by McNutt et al. (1990) were used for $^{87}Sr/^{86}Sr$ analysis, via thermal ionization mass spectroscopy with an analytical precision value of (±0.0001). The $\delta^{37}Cl$ was determined using the method described in Eggenkamp (1994) and Shouakar-Stash et al. (2005a). The $\delta^{81}Br$ was determined using the method described in Shouakar-Stash et al. (2005b). Analyses were performed on CH_3Cl for $\delta^{37}Cl$ and CH_3Br for $\delta^{81}Br$ with a precision of 0.1‰ for both isotopes.

3.2. Mass balance mixing model

To provide quantitative information on groundwater mixing, a solute-weighted mass balance mixing model was performed using isotopes and solutes that behave conservatively. Recharge water, deep saline groundwater, and seawater were used to investigate the recharge and salinization source(s) for the Wadi Watir delta alluvial aquifers because they are representative end members. The isotopic values of $^{87}Sr/^{86}Sr$, $\delta^{37}Cl$, and $\delta^{81}Br$, as well as Cl and Br concentrations in different end members, were used in the mass balance equation to estimate mixing fractions in the final groundwater (Faure, 1986). The average isotopic signatures and chemistry of recharge water (R) at sites $At_{1,2}$, Mc, and F_1 were calculated to mimic the recharge water that comes from the watershed catchment. The highest groundwater salinity and chloride concentrations (TDS = 24,975 mg/l; Cl = 13,186 mg/l: SM 1) were recorded at site S, a deep drilled well located in the well field (Total depth = 68 m). This site was selected to represent the deep saline groundwater. Modern seawater was represented by a sample collected from the Gulf of Aqaba (site G). The ternary solute-weighted mass balance equation (Clark, 2015) has been used with different implicit mixing percentages of three end members ranging from 0 to 100% to investigate the main source(s) of groundwater recharge and salinization as follows:

$$F_{(T)} = f_1 + f_2 + f_3 = 1 \quad (1)$$

$$Cl_{(T)} = f_1 Cl_1 + f_2 Cl_2 + f_3 Cl_3 \quad (2)$$

$$\delta X_{(T)} = f_1 \delta X_1 + f_2 \delta X_2 + f_3 \delta X_3 \quad (3)$$

(X refers to Sr, Cl or Br isotopes)

$F_{(T)}$, $Cl_{(T)}$ and $\delta X_{(T)}$ are the sum of total mixing fractions, chloride (or bromide) concentration (mg/l), and isotopic signature values (‰), respectively; $Cl_{1,2,3}$ and $X_{1,2,3}$ are the chloride concentration (mg/l) and isotopic signature values (‰) in each end member, respectively; and f_1, f_2, and f_3 are the anticipated mixing fractions from different end members. In cases of a simple conservative mixing ratio of two end members, f_3 is considered to be zero. Equations (1)–(3) can be solved using Excel Solver or trial and error to estimate accurate mixing ratios of each member (f_1, f_2, and f_3).

3.3. Solute transport and flow model

The computer program SEAWAT (Guo and Langevin, 2002) was used for groundwater flow and transport modeling because it can simulate three-dimensional variable-density groundwater flow in porous media and seawater intrusion into coastal aquifers. This program combines a groundwater flow model, MODFLOW (Harbaugh et al., 2000) with a solute transport model, MT3DMS (Zheng and Wang, 1999), into a single program that solves the density-dependent groundwater flow and solute-transport equations derived by Guo and Langevin (2002).

4. Results and discussions

4.1. Groundwater geochemistry

Groundwater chemistry was obtained from deep and shallow wells completed in the Quaternary alluvial aquifers (SM 1). Groundwater in the aquifers of the Wadi Watir delta contain total dissolved solids (TDS) that range from 942 (site 51) to 24,975 (site S) mg/l. High groundwater salinity was recorded in the main well field (site S) and near the coast (sites 35 and 42). Chloride and bromide concentrations were used to investigate the mechanisms that lead to groundwater salinization in the delta alluvial aquifers. These halogens have a uniform ratio in seawater and are considered to be good conservative markers for determining groundwater

Table 1
Isotope analyses ($^{87}Sr/^{86}Sr$, $\delta^{37}Cl$) for rock samples from different aquifers in the Wadi Watir watershed.

Locality Area	Site Map	Rock Type	Aquifer	Rock Age	$\delta^{37}Cl$ (‰)	$^{87/86}Sr$
Wadi El Ain	An_1	Granite (Basement Rocks)	Basement	Precambrian (Younger Granite)	−0.20	0.71,557
	An_2	Granite (Basement Rocks)	Basement	Precambrian (Younger Granite)	−0.58	0.72,182
Main Channel	Up.Cr	Limestone	Upper Cretaceous	Upper Cretaceous	1.41	0.70,835
	L.Cr	Sandstone	Lower Cretaceous (Nubian sandstone)	Lower Cretaceous	−0.22	0.70,788
	O.Gr[a]	Granite (Basement Rocks)	Basement	Precambrian (Older Granite)	–	0.70,290
	Mc_1	Granite (Basement Rocks)	Basement	Precambrian (Younger Granite)	−0.62	0.71,330
	Mc_2	Granite (Basement Rocks)	Basement	Precambrian (Younger Granite)	0.15	0.70,854
Furtaga Springs	F_1	Granite (Basement Rocks)	Basement	Precambrian (Younger Granite)	−0.12	0.71,206
	F_2	Granite (Basement Rocks)	Basement	Precambrian (Younger Granite)	−0.57	0.71,780
	F_3	Granite (Basement Rocks)	Basement	Precambrian (Younger Granite)	−0.69	0.71,228

Note: Locations for the rock samples are shown in Fig. 2a.
[a] $^{87/86}Sr$ analyses for the older granitic rocks are from after (Bielski, 1982).

mixing, salinization origin, and recharge sources (Du et al., 2015; Vengoush, 2014; Stotler et al., 2010). A simple mass balance mixing model was developed using the chloride and bromide concentrations in the recharge water (R) and gulf of Aqaba seawater (G) as end members (see section 3.2 and SM 1). In Fig. 1S (Supporting Material), most of the groundwater samples do not fall along the seawater dilution mixing line as they have different observed Cl/Br ratios, with ratios ranging from approximately 50 to 97. This ratio range strongly suggests that groundwater salinity is not related to mixing with modern seawater (Gulf of Aqaba Cl/Br = 287).

To gain insight into the source(s) of groundwater salinity, the Cl/Br ratios were plotted against Cl for all groundwater samples along with end member waters of recharge water, Gulf of Aqaba seawater, sabkha groundwater, and evaporated ancient seawater. Fig. 3 shows that shallow and deep groundwater samples fall between two end members: the recharge water from the watershed and evaporated ancient seawater (Collins (1975), which is similar to sabkha water (Gavish, 1974). Evaporated seawater is from the salt-water invasion layer of marine origin (sandstone intercalated with clay layer overlying the bedrock; Fig. 2b), and this highly saline groundwater mainly originated from three sequential sea transgressions and regressions during the Pleistocene epoch (Abbas et al., 2004; Mabrouk and Nasr, 1997). The fresh groundwater in the Wadi Watir delta aquifers has been affected by mixing with this older deep saline groundwater that is approximately 2400–3600 years old (Eissa et al., 2013a). The Cl concentration and Cl/Br ratio data confirm that groundwater salinization in the Wadi Watir delta aquifers primarily originates from upwelling of a deep saline groundwater, which is caused by overpumping.

According to Sulin (1946), groundwater can be classified into two main groups based on ion ratios (ion ratio [r] is the ratio of the ion to total cations or total anions in meq/l). Groundwater is divided into water types based on an rNa/rCl ratio [(Na(epm)/Total Cations)]/[Cl(epm)/Total anions] > 1 or < 1. According to Sulin (1946) and Schoeller (1962), the former case (>1) is subdivided into two fundamental water types. A ratio of [rNa - rCl]/[rSO_4] > 1 indicates an Na:SO_4 water type, whereas a ratio of [r(Na + K) - rCl]/[rSO_4] < 1 indicates a Na:HCO_3 water type. In the latter case (<1), a ratio of [rCl - r(Na + K)]/[rMg] < 1 indicates an Mg:Cl water type, whereas a ratio of [rCl - r(Na + K)]/[rMg] > 1 indicates a Ca:Cl water type.

Four samples have a ratio of [rNa/rCl] > 1 so they represent an Na:SO_4 water type (sites 19, 36, 38, and 51). These groundwaters have relatively low salinity and their chemistry is primarily derived from terrestrial salt leaching and/or rock-water interactions. The majority of groundwater samples have a ratio of [rNa/rCl] < 1 and are characterized by Ca:Cl or Mg:Cl water types. Deep drilled wells (sites 17–22), a dug well located close to these wells (site 45), and two dug wells located along the coast (sites 35 and 42) are Ca:Cl water types. The deep drilled wells with high pumping rates contain Ca:Cl type groundwater because of upwelling of a deep saline groundwater of old marine origin. Shallow dug wells with low to moderate pumping rates generally contain a Mg:Cl type groundwater. This water type is derived primarily from leaching of upper Cretaceous carbonate rocks of marine origin that are embedded in the alluvial clastic deposits (Fig. 2a).

4.2. *Groundwater origin and salinization processes*

The $\delta^{18}O$ and $\delta^{2}H$ values of groundwater in the main well field area are similar to the isotopic composition of the shallow groundwater in the alluvial aquifers of the Wadi Watir delta (Eissa, 2012; Abuelfadl, 2004). Thus, the potential mixing of a deep saline groundwater and shallower groundwater in the well field area cannot be uniquely determined using these isotopic tracers. In this study, $^{87}Sr/^{86}Sr$, $\delta^{37}Cl$, and $\delta^{81}Br$ isotopic data are combined with major-ion chemistry to address the origin of groundwater and groundwater salinization in the Wadi Watir delta aquifers.

4.2.1. *Strontium isotopes ($^{87}Sr/^{86}Sr$)*

The $^{87}Sr/^{86}Sr$ in groundwater is controlled by water-rock interactions and reflects the isotopic signature of strontium-containing minerals in aquifers (Lyons et al., 1995). The isotopic ratio of $^{87}Sr/^{86}Sr$ in water has been used to determine the geochemical history of groundwater (water-rock interactions), groundwater mixing, groundwater recharge sources, and sources of salinity (McNutt et al., 1984; Lyons et al., 1995; Clark and Fritz, 1997).

In the Wadi Watir catchment and delta area, $^{87}Sr/^{86}Sr$ in

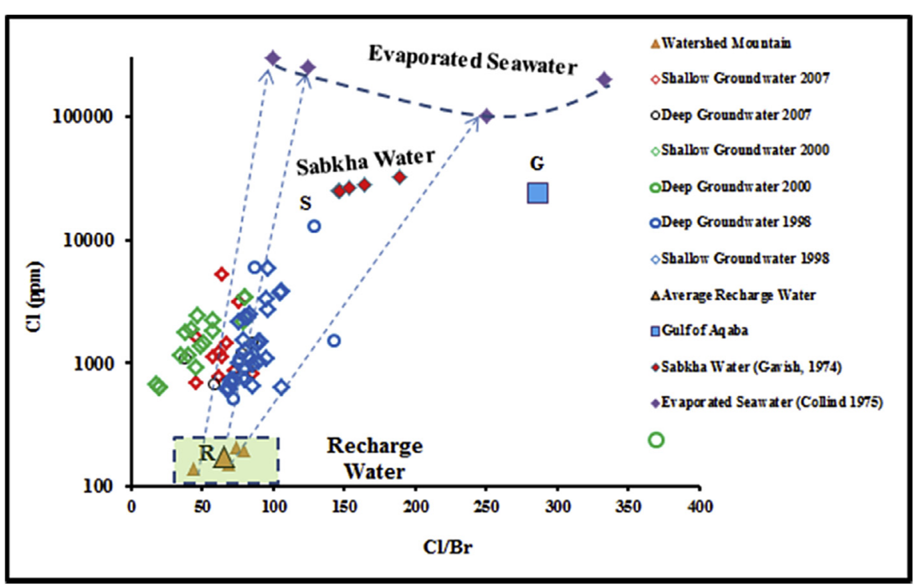

Fig. 3. Chloride concentrations (mg/l) versus Cl/Br ratios in groundwater from the recharge area watershed catchment (Watershed Mountain) and Wadi Watir delta aquifers. Groundwater samples collected in 1998, 2000, and 2007 are from Abuelfadl (2004), Abd El Hafez (2001) and Eissa et al. (2013a,b), respectively. G is Gulf of Aqaba seawater and S is the highest salinity groundwater sample from the main well field.

groundwater ranges from 0.70,698 (site 17) to 0.70,823 (site An_3), and seawater from the Gulf of Aqaba has a value of 0.70,925. Lower $^{87}Sr/^{86}Sr$ values were measured in groundwater samples from the main well field, whereas higher $^{87}Sr/^{86}Sr$ values were measured in groundwater samples from the watershed catchment (sites $At_{1,2}$, Mc, and $An_{1,2,3}$).

The higher $^{87}Sr/^{86}Sr$ values for groundwater in the watershed catchment area (Watershed Mountain) at sites $At_{1,2}$, Mc, and $An_{1,2,3}$ indicate water-rock interaction with younger granitic rocks that have high $^{87}Sr/^{86}Sr$ values (Table 1, Fig. 4). In contrast, Furtaga Springs issues mainly from older granitic rocks and has a lower $^{87}Sr/^{86}Sr$ value. The $^{87}Sr/^{86}Sr$ value of these springs is within the range of the average $^{87}Sr/^{86}Sr$ content of the older granitic (O.Gr), upper Cretaceous limestone (Up.Cr), and lower Cretaceous sandstone (L.Cr) rocks that outcrop in the upper watershed (Fig. 2a). Older granitic rocks in the Sinai Peninsula are subduction-related granites formed by the partial melting of mafic gneiss or amphibolite, so they have a low $^{87}Sr/^{86}Sr$ value that is around 0.7029 (Arth and Hanson, 1975; Bielski, 1982).

A solute-weighted mass balance mixing model was developed using three end member waters, as described in section 3.2. A mass balance mixing line that extends from the average recharge water (R) through deep groundwater samples collected in 2007 at sites 17, 19, and 21 is extrapolated with the same slope to estimate the $^{87}Sr/^{86}Sr$ isotopic signature of a deep saline groundwater end member in the same area as these wells, which is represented by a groundwater sample at site S with a high chloride concentration (13,186 mg/l).

All $^{87}Sr/^{86}Sr$ values for groundwater samples from the Wadi Watir delta aquifers fall within the three end member mixing lines developed using the average recharge water (R), deep saline groundwater (S), and Gulf of Aqaba seawater (G) values. The $^{87}Sr/^{86}Sr$ values for shallow groundwater (hand-dug wells) in the Wadi Watir delta alluvial aquifers are similar to the isotopic value of the average recharge water that comes from the watershed catchment (Fig. 2a). Furtaga Springs (F_1) and site 35 represent the initial (most dilute) and final (highest chloride concentration) end members of shallow groundwater evolution from leaching and dissolution of the aquifer rock matrix. These data strongly support the hypothesis that groundwater from the upper watershed catchment area (sites $At_{1,2}$ and Mc), that flows through the main channel (site F_1), is the primary source of groundwater recharge supplying the Wadi Watir delta aquifers (El Ghazawi, 1999; El Sayed, 2006; Eissa et al., 2013a,b).

Groundwater from the deep drilled wells (sites 17, 19, 21, and 23) in the main well field has lower $^{87}Sr/^{86}Sr$ values compared with other groundwater in the study area (Fig. 4b). Deep groundwater is in contact with older granitic bedrock and boulders and clastic alluvium (Fig. 2b). Consequently, groundwater has lower $^{87}Sr/^{86}Sr$ values because of the water-rock interaction in which the Sr isotope exhibits no detectable fractionation by any natural processes (Stober and Bucher, 2002). The $^{87}Sr/^{86}Sr$ data shows that groundwater from the deep drilled wells in the main well field is a mixture of upwelling saline water with lower $^{87}Sr/^{86}Sr$ values, and groundwater recharge from the upper watershed with higher $^{87}Sr/^{86}Sr$ values.

The coastal groundwater sites 34, 35, and 42 have high groundwater salinity and chloride content, which indicates potential seawater intrusion and/or potential upwelling of deep saline groundwater (Fig. 4b). $^{87}Sr/^{86}Sr$ values indicate that the source of increased salinity in these coastal groundwaters can be from either seawater intrusion or upwelling of a deep saline groundwater.

Solving equations (1)–(3) using chloride concentrations and $^{87}Sr/^{86}Sr$ values produces mixing fractions of the end member waters, which are groundwater recharge, a deep saline groundwater, and Gulf of Aqaba seawater. For deep wells in the main well field (sites 17, 19, 21, and 23) increased salinity in these groundwaters was derived from 4.0 to 10.2% upwelling of a deep saline groundwater (Table 2). For shallow wells located along the coast with increased salinity (sites 34, 35, and 42), the increased salinity is derived from a mixture of 18–28.8% of an upwelling deep saline groundwater and 2.2–5.5% of seawater intrusion from the Gulf of Aqaba into the shallow alluvial aquifers.

4.2.2. *Chloride isotopes ($\delta^{37}Cl$)*

The main factors responsible for $\delta^{37}Cl$ values in groundwater are

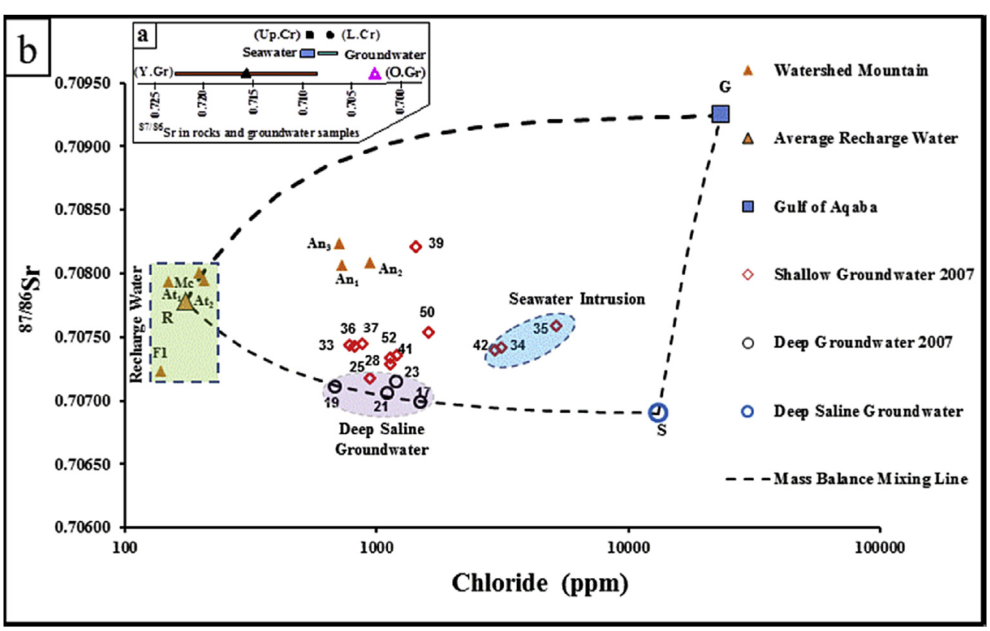

Fig. 4. a) $^{87}Sr/^{86}Sr$ values for rocks, groundwater, and seawater in the study area (Table 1 and SM 1). b) $^{87}Sr/^{86}Sr$ versus chloride concentration in groundwater, the most saline deep groundwater (S), and seawater from the Gulf of Aqaba (G). The groundwater site locations are shown in Fig. 1. The rock sample locations (Up.Cr, L.Cr, O.Gr, and Y.Gr) are shown in Fig. 2a.

Table 2
Calculate mixing fractions of end member waters for higher salinity groundwater in deep drilled wells located in the main well field and in shallow wells along the coast.

Well No.	Estimated mixing Percentage (%)			Well No.	Estimated mixing Percentage (%)		
	(G)	(R)	(S)		(G)	(R)	(S)
17	0	89.8	10.2	34	2.2	79	18.8
19	0	96	4	35	2	80	18
21	0	92.7	7.3	42	5.5	65.7	28.8
23	0	92.2	7.8				

G, R, and S denote seawater, recharge water, and deep saline groundwater, respectively.

rock-water interactions and mixing of waters with different $\delta^{37}Cl$ compositions (Shmulovich et al., 1999; Liebscher et al., 2006a, 2006b).

In the Wadi Watir delta alluvial aquifers, $\delta^{37}Cl$ ranges from −0.85‰ (site 52) to +0.22‰ (site 17) relative to Standard Mean Oceanic Chloride (SMOC = 0‰, Kaufmann et al., 1984). The Gulf of Aqaba seawater (G) has a value of −0.01‰. The solute-weighted mass balance mixing model indicates that groundwater located in the up gradient catchment area is the main source of groundwater recharge (sites $At_{1,2}$, F_1 and Mc) to the delta alluvial aquifers. This groundwater has low $\delta^{37}Cl$ values ($-0.42‰ < \delta^{37}Cl < -0.06‰$) (Fig. 5).

The majority of shallow groundwater (hand-dug wells) in the Wadi Watir delta alluvial aquifers has a $\delta^{37}Cl$ isotopic signature that is within the range of the recharge water that comes from the up gradient catchment (Watershed Mountain; Fig. 5). The $\delta^{37}Cl$ and chloride concentration both increase down groundwater flow paths in the study area from the recharge area (R) to the delta alluvial aquifers. Shallow groundwater $\delta^{37}Cl$ values are similar to that of felsic granitic, lower Cretaceous (sandstone), and upper Cretaceous (limestone) rocks (Table 1 and Fig. 5a; b). The $\delta^{37}Cl$ signature of the shallow groundwater primarily reflects leaching and dissolution of the aquifer matrix (Eggenkamp, 1994; Frape et al., 2004), which mainly consists of upper Cretaceous felsic granitic and marine carbonate boulders embedded in the aquifer matrix (El Kiki et al., 1992).

The deep drilled wells in the main well field (sites 17, 19, 21, and 23), and one shallow dug well located along the coast (site 35), are characterized by higher $\delta^{37}Cl$ values than all other groundwaters in the study area. The high $\delta^{37}Cl$ values in the main well field groundwater are caused by the upwelling of a deep saline water that is in contact with old evaporated marine deposits beneath the freshwater lens in the well field. The first salt to be deposited during evaporation of saline water is generally enriched in $\delta^{37}Cl$ (more positive values), whereas salt deposited later has more negative $\delta^{37}Cl$ values (Eggenkamp et al., 1995). The $\delta^{37}Cl$ record in marine salt deposits varies considerably in stratigraphic units of different ages, from −0.5 to +0.5‰ relative to SMOC (Eastoe et al., 2007; Shouakar-Stash, 2008). The difference between the values of $\delta^{37}Cl$ in seawater and the deep saline groundwater is 0.27‰, which is approximately two times the maximum standard deviation measurement precision error (stdev = 0.13). Therefore, mixing ratios from different end members have not been estimated using this isotope.

4.2.3. Bromide isotopes ($\delta^{81}Br$)

The natural distribution of $\delta^{81}Br$ has only been reported for sedimentary formation waters, and the fractionation processes are poorly understood (Stotler et al., 2010). Eggenkamp and Coleman (2000) were the first scientists since 1920 to report $\delta^{81}Br$ values of natural samples with good precision. Shouakar-Stash et al. (2005a) subsequently presented a method for determining $\delta^{81}Br$ with excellent precision and accuracy that used continuous-flow mass spectrometry with seawater as the standard. $\delta^{81}Br$ in groundwater in the study area ranges from +0.22‰ (site 19) to +1.28‰ (site Mc), relative to Standard Mean Oceanic Bromide (SMOB), and seawater from the Aqaba Gulf is +0.57‰ relative to SMOB. Groundwater in the Wadi Watir watershed recharge area (sites F_1, At_2, and Mc) has low bromide concentrations (2.5–3.2 mg/l) and high $\delta^{81}Br$ values (+0.94 to +1.28‰) as compared to groundwater in the Wadi Watir alluvial aquifers (Fig. 6). Dilute recharge area groundwaters have $\delta^{81}Br$ values similar to those observed for freshwater (+0.5 to +1.2‰), as reported by Shouakar-Stash (2008).

Shallow groundwater in the delta alluvial aquifers has lower

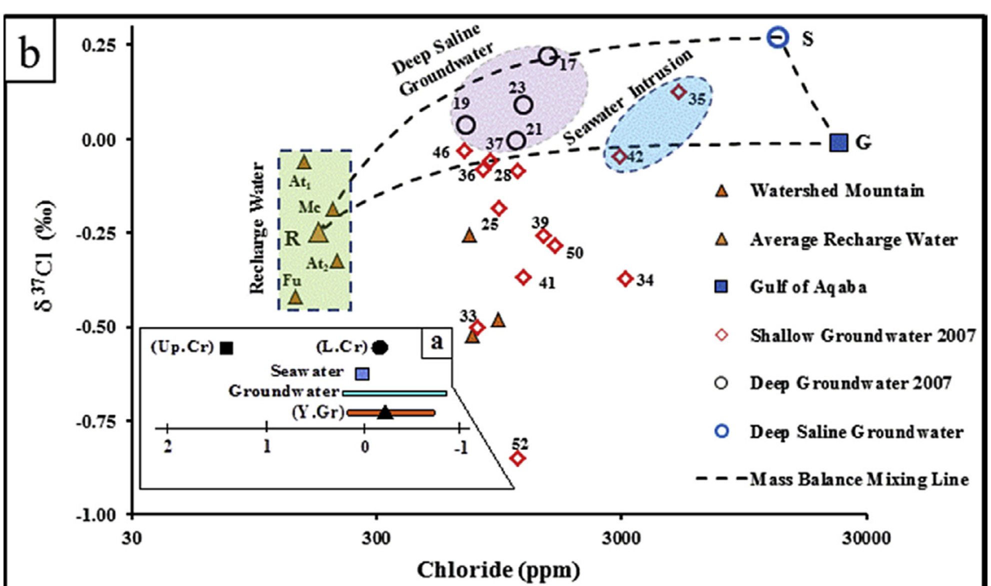

Fig. 5. $\delta^{37}Cl$ versus Cl concentration for groundwaters, a deep saline groundwater (S), and Gulf of Aqaba seawater (G). The groundwater site locations are shown in Fig. 1 and the data are presented in SM 1. The Up.Cr, L.Cr, and Y.Gr rock sites are shown in Fig. 2a and presented in Table 1.

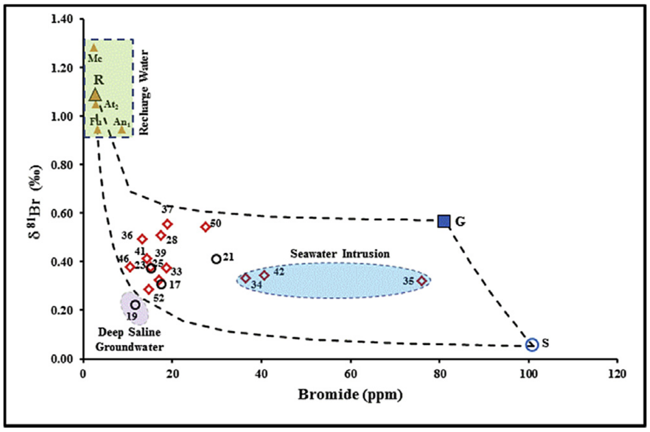

Fig. 6. δ^{81}Br ‰ (SMOB) versus Br concentration (mg/l). Groundwater site locations are shown in Fig. 1 and data are presented in SM 1.

δ^{81}Br values than both recharge groundwater and Aqaba Gulf seawater (Fig. 6; site G). Samples from two of the drilled wells in the main well field (sites 17 and 19) have two of the three lowest δ^{81}Br values for groundwater in the study area. The lower δ^{81}Br values of these two samples are primarily caused by the upwelling of saline groundwater that comes in contact with evaporated marine deposits beneath the well field (Fig. 6). The recharge water (R) to deep saline water (S) mixing line was interpolated to estimate the δ^{81}Br value of site S groundwater, which had a high bromide concentration (101 mg/l). This extrapolated δ^{81}Br value of about 0.1‰ is within the range of δ^{81}Br isotope values (−0.3 to +0.27‰) for water in a deep water formation that is in contact with evaporated seawater at the Siberian Platform (Shouakar-Stash et al., 2007), and is similar to a deep saline water in the Quaternary coastal plain aquifer in Laizhou Bay, China (−0.68 to −0.16‰), which also has an overlying fresh water lense with a δ^{81}Br value of +0.35‰ (Du et al., 2015) similar to that of the fresh water lense in this study area. Samples from wells along the coast (sites 34, 35 and 42) plot between the shallow groundwater and the Gulf of Aqaba (G) and/or deep saline water δ^{81}Br values and Br concentrations, which indicates that these waters have likely been influenced by seawater intrusion and/or mixing with a deep saline water.

4.3. Solute-transport and flow dynamics model

Solute transport modeling was performed using observed chemistry and water level (head) data to: (1) simulate potential sea water intrusion along the coast, (2) simulate vertical movement and migration of deep saline groundwater into shallower aquifers caused by overpumping in the main well field, (3) estimate recharge rates from the mountain blocks into the alluvial aquifers, and (4) refine pumping rates for the Wadi Watir delta alluvial aquifers. Model results were compared to and calibrated using observed seawater intrusion along the coast (identified using water chemistry and isotopic data), salinity increases in the main well field water, estimated groundwater recharge from an earlier study (Eissa et al., 2013a), and observed pumping data.

4.3.1. Governing equations and model framework

SEAWAT (Guo and Langevin, 2002; Langevin and Guo, 2006), a program for simulating water flow with variable density, was used to simulate the migration of solutes from a deep saline source into the shallow alluvial aquifers and seawater intrusion along the coast. Solute transport in porous media includes the advection, molecular diffusion, and mechanical dispersion described by Zheng and Bennett (1995), which can be calculated using the following partial differential equation:

$$\frac{\partial C}{\partial t} = \nabla.(D\nabla C) - \nabla.(\nu C) - \left(\frac{q}{\theta}\right)Cs + \sum_{K=1}^{N} R_k \tag{4}$$

where, $\partial C/\partial t$ is the changing of groundwater concentration (C [ML^{-3}]) with time (t), D is the hydrodynamic dispersion coefficient (L^2T^{-1}), C is the solute concentration (mg/l), Cs is the solute concentration of the recharge water (mg/l), ν is the water velocity (LT^{-1}), and R_k is the rate of solute production or decay.

In this study, the R factor was not included (R = 0) because the model is a solute transport nonreactive model. Baxter and Wallace (1916) developed the empirical relationship between the densities and concentration of fresh water, deep saline water, and seawater concentrations described in the following equation:

$$\rho = \rho f + EC \tag{5}$$

where, E is a dimensionless constant factor that is a function of the salt concentration (ML^{-3}), and ρ and ρ_f are the densities of seawater and fresh water, respectively (ML^{-3}). The slope $E = \frac{\partial\rho}{\partial C}$ has a value of 0.7143 for the range of fresh (recharge) water and seawater.

The SEAWAT program depends on the concept of a fresh-water equivalent head in a saline groundwater or seawater environment (Guo and Langevin, 2002) according to the following equation:

$$h = \frac{\rho f}{\rho}hf + \frac{\rho - \rho f}{\rho}Z \tag{6}$$

where, h is the saline or seawater head (L), h_f is the equivalent fresh-water head (L), ρ_f is the density of fresh water (ML^{-3}), ρ is the density of seawater (ML^{-3}), and Z is elevation (L). If sea level is used as the standard, Z will equal zero, which makes the second term of the equation equal to zero so that the equation can be simplified to:

$$h = \frac{\rho f}{\rho}hf \tag{7}$$

The parameters and data used for the simulations are summarized in Table 3. The model boundaries were selected to be: (1) the Gulf of Aqaba to the east, (2) the mountain block alluvial contact to the west, and (3) the mountain block alluvial contact where the western block meets the Gulf of Aqaba to the north and south. A finite-difference grid oriented along the north-south and east-west axes of the Wadi Watir delta was used for the model. There are 60 columns and 120 rows with uniform grid spacing of 98 m in both directions (Fig. 7a). In the vertical direction, the model grid consists of 27 layers that represent the five hydrostratigraphic units of the Wadi Watir delta aquifers (Fig. 2b). Model layers 1 to 12 correspond to layer A1 (Fig. 7a; b), which contains the top three hydrostratigraphic units that are comprised of surficial alluvial deposits and sandy clay and have a hydraulic conductivity of 4 m/day (Eissa et al., 2013a). Layers 13 through 18 correspond to layer A2, which contains the fourth hydrostratigraphic unit beneath the land surface, which is comprised of sands and gravels and has a hydraulic conductivity of 11 m/day (El-Refaei, 1992). Layers 19 to 27 correspond to layer A3, which contains the fifth hydrostratigraphic unit beneath the land surface and is primarily comprised of sand intercalated with clay and has a hydraulic conductivity of 10^{-3} m/day (Fetter, 2001). Land surface elevations used in the model are from the Digital Elevation Model STRM-90 m (U.S. Geological Survey, 2004) coupled with 22 ground elevation surveyed spots that represent the wells. The model layer thickness was taken from the geoelectrical cross section of Abbas et al. (2004).

Table 3
Parameters of the groundwater flow and transport model for the Wadi Watir delta alluvial aquifers.

Parameter	Model value
Hydraulic Conductivity (m/day)	4 m/day for Layer A1; 11 m/day for Layer (A2) and 10^{-3} m/day for Layer A3 (Eissa et al., 2013a) ($K_x = K_y = 10K_z$)
Total Porosity	30% (Khalil, 2010)
Longitudinal Dispersivity	$\alpha_L = 100$ m (Gelhar et al., 1992)
Longitudinal (α_L)/Horizontal (α_T)	$\alpha_L/\alpha_T = 0.1$ $\alpha_T/\alpha_V = 0.01$
Molecular Diffusion Coefficient (m^2/day)	10^{-9} m^2/day
Storage Coefficient	3.14×10^{-4} (Himida, 1997)
Density/Concentration Slope $\boldsymbol{E} = \partial\rho/\partial\boldsymbol{C}$	0.7143 (Baxter and Wallace, 1916)

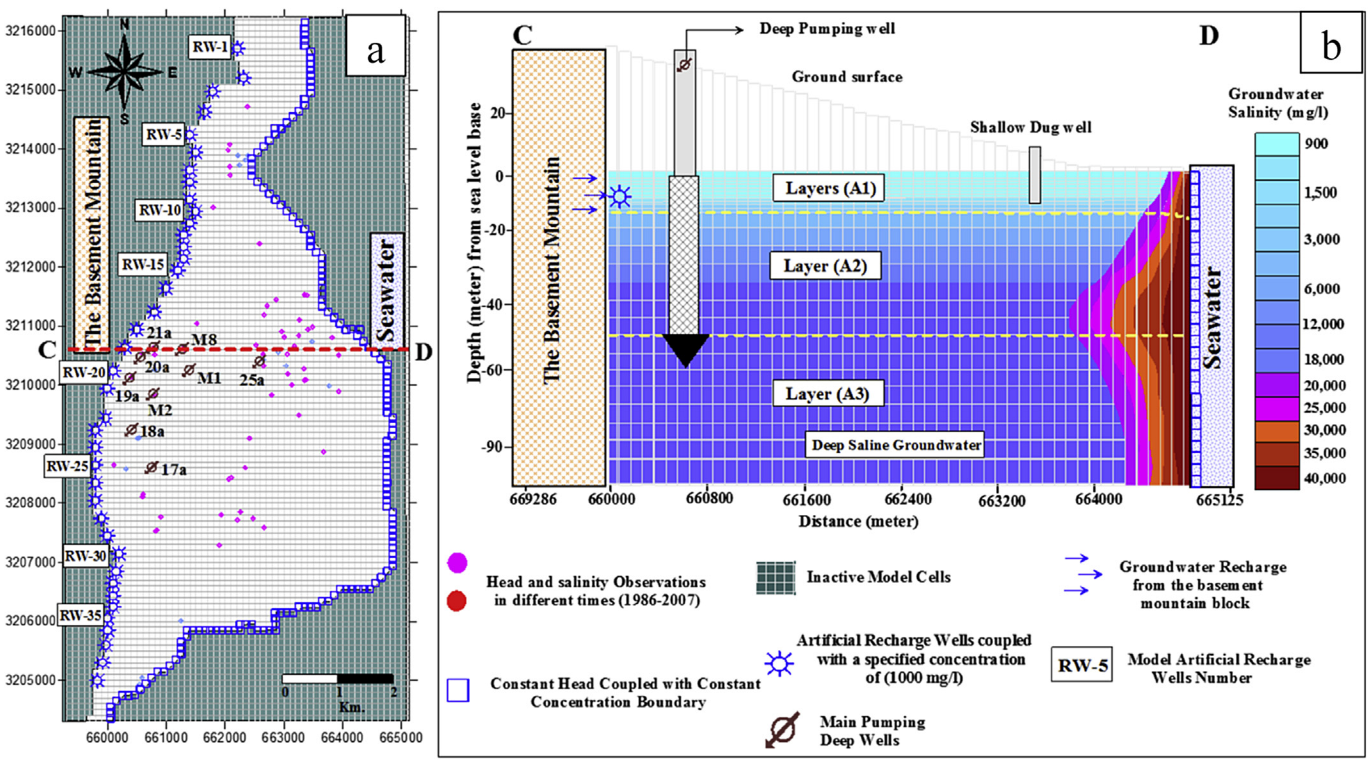

Fig. 7. The finite difference grid cells, boundaries, and observations used for the SEAWAT model: a) in the *x* and *y* directions; b) in the *z* direction.

4.3.2. Model parameters, boundary conditions, and internal sinks

The model parameters are summarized in Table 3. The longitudinal dispersivity is assumed to be homogeneous in the flow system, and is set at 100 m based on the overall model scale of 4000 m (Gelhar et al., 1992). The boundary conditions for both flow and transport are shown in Fig. 7. The model base is assumed to be a no-flow boundary and is represented by the consolidated granitic basement. For the flow model, a constant head boundary is set to sea level at the coast, which represents the mean seawater level at the shore line of the Gulf of Aqaba (Fig. 7a). A constant concentration boundary was applied for the 27 model layers at the coast and this concentration was assumed to be 41,000 mg/l, based on a gulf water sample analysis (Eissa et al., 2013b). This concentration value corresponds to a fluid density of 1042 kg/m^3, according to Equation (5). The Wadi Watir delta alluvial aquifers are primarily recharged from the mountain block aquifer along the western boundary of the groundwater flow model area. The boundary between the mountain block and the unconsolidated delta aquifers is simulated by coupling the injection recharge wells (RW-1 to RW-39 in Fig. 7a) with a specified concentration boundary set of 1000 mg/l. The screened intervals are placed within the subsurface fresh recharge zone represented by El-Refaei (1992) at a depth of 40–45 m below land surface. The salinity value of 1000 mg/l for the groundwater recharge is based on an average from three samples collected from Furtaga Springs, which are near the mountain front-alluvial aquifer boundary (Fig. 1a) (Eissa, 2012). This concentration value corresponds to a fluid density of 1001 kg/m^3 according to Equation (5). Rainfall on the Wadi Watir delta is minimal (35 mm/year), so any potential groundwater recharge from rainfall on the delta is not included in the model.

4.3.3. Initial conditions

Because the boundary conditions for both flow and transport have been adjusted (Fig. 8a), initial water levels were specified for the groundwater flow model by interpolating the known values of water levels in February 1986 (El Kiki et al., 1992) using ordinary Kriging. Steady-state conditions for the groundwater flow and solute transport models were obtained using long-term transient simulations under arbitrary initial conditions until system stabilization and equilibrium for salinity (TDS) and physical flow were reached within the models. The $^{87}Sr/^{86}Sr$, $\delta^{37}Cl$, and $\delta^{81}Br$ data support the presence of a deep saline groundwater beneath the main well field and close to the coast, which originates from the sandstone intercalated with clay layer shown in Fig. 2, so the equilibrium salinity was modified to include a high-salinity feature at depth. El-Refaei (1992) measured the salinity with depth in a drilled well located adjacent to the main well field. The salinity of groundwater in this drilled well reached 18,000 mg/l at a depth of 34 m below sea level (Fig. 7b). Simulations were carried out for the entire period of available data (1982–2009). The steady-state outputs for water level and salinity were used as the initial conditions for the transient simulation that represents aquifer pumping. To simulate the upwelling of deep saline groundwater, pumping rates for the drilled wells of the main well field were obtained from the well site engineer (Eissa et al., 2013a). The pumping rates of these wells varied throughout the period of 1982–2009 depending on groundwater availability, which was related to flash flood intensity and/or frequency. Because of known uncertainties in the recorded pumping rates for production wells, these rates were adjusted during calibration to ± 20% of the reported value. Within the model, each well was assigned an individual withdrawal rate that was specific for each stress period. The total withdrawal rate is for the group of wells that comprise the main well field located at the outlet of the Wadi Watir watershed where it enters the delta (Fig. 1b). The pumping rate for hand-dug wells is unknown, so it was initially assumed to be 5 m^3/day based on discussions with well owners during field trips. Pumping rates for hand-dug wells were adjusted during calibration.

4.3.4. Simulation of subsurface recharge and upwelling of saline groundwater

Subsurface groundwater recharge to the Wadi Watir delta alluvial aquifers was evaluated using the SEAWAT model developed for this study. The model was calibrated in a transient state, in which salinity was tied to head (water level) observations for different time periods and the induced pumping stresses from 1986 to 2009. A total of 58 head observations were used for the period from 1982 to 2007 (SM 2), and a total of 94 salinity observations were used for the period of 2005–2007 (SM 3). Forty one salinity observations were selected based on the availability of $\delta^{18}O$ and δ^2H data (Abuelfadl, 2004; Eissa et al., 2013a,b) in order to correct TDS values of samples affected by evaporation. The TDS was corrected by estimating the evaporation factor (F) using the Rayleigh distillation equation (Gonfiantini, 1986) of $\delta^{18}O$ and δ^2H, to calculate the pre-evaporative concentration values. The estimated evaporation factor (F) ranged between 1 and 1.92 and high evaporation factors were only detected in large diameter, hand-dug wells. The normalized salinity (TDS_N) was estimated as shown in SM 3, where $TDS_N = [TDS_{Obs}/F]$ and TDS_{Obs} refers to the observed groundwater salinity measured in the field.

Model calibration was achieved through trial and error by adjusting the values of recharge injected into recharge wells at the boundary between mountain blocks and the alluvial aquifer (Fig. 7a) until general agreement between the calculated and measured water levels and salinity were reached (Figs. 8 and 9). Model calibration was obtained when a reasonable value of relative

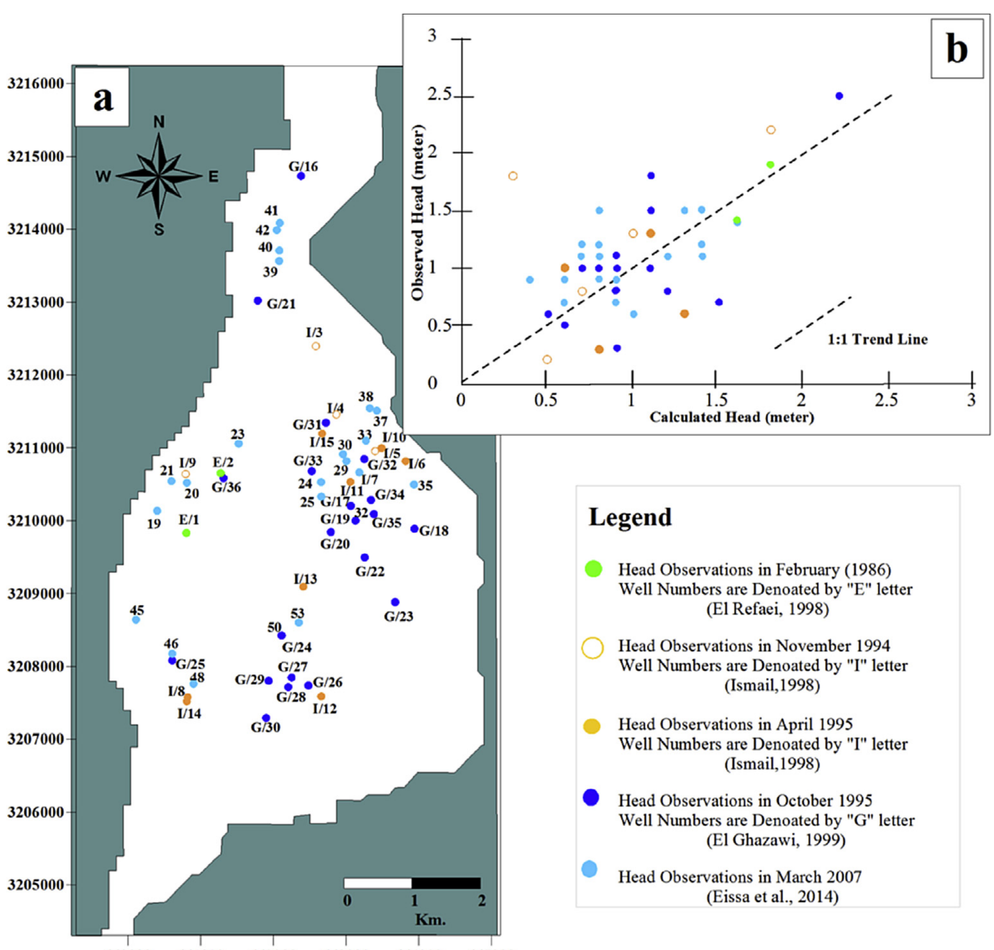

Fig. 8. a) Well location map for water level (head) observations. B) Calculated versus observed water levels. The data are presented in SM 2.

error [Relative Error = 1/N x [Absolute ($H_{Obs} - H_{Calc}$)/($H_{Max} - H_{Min}$)] between the modeled and observed water level was less than 14%; N, H_{Obs}, and H_{Calc} denote the number of head observations, field observed, and modeled calculations, respectively. A dispersivity value of 100 m was found to yield the best agreement between calculated and observed salinity and it is consistent with the hydrogeology of the area scale (Gelhar et al., 1992). The pumping rates were also estimated using this model by changing the pumping rates until the salinity breakthrough curve of the calculated values matched the observed values (Fig. 10). Based on the pumping stresses, the calibrated model simulates the transient changes in groundwater levels and salinity migration. Using both head and salinity observations resulted in a more accurate estimate of recharge and a better understanding of solute migration from the deep layers into the fresh-water lens of the shallow aquifers. The modeled salinity curves for sites 18, 19, 34, and 35 have different shapes and slopes because of different pumping stresses and rates through the modeled time period, starting from steady state conditions in 1982 until 2009 (Fig. 10). The contour shaded lines and breakthrough salinity curves clearly show that groundwater salinity is mainly controlled by pumping rates that are linked with an upwelling of deep saline water that mixes with the fresh-water lens.

The estimated pumping rates are consistent with the well type. Pumping rates for the drilled wells ranged from 200 (site 20) to 1400 m^3/day (site M2) (Fig. 7a). Pumping rates for the hand-dug wells varied considerably, from 0.5 to 7 m^3/day for all wells except No. 35, which attained a pumping rate of 30 m^3/day. The total estimated average pumping rate for the main well field was 3100 m^3/day and for the shallow hand-dug wells was 60 m^3/day for 1982 to 2009 (Eissa et al., 2013b).

Average recharge from the mountain blocks to the delta alluvial aquifers ranged from 3900 m^3/day (1982–1987) to 7770 m^3/day (1987–2002), with an average rate of 6000 m^3/day for 1982 to 2009 (SM 4). Most of the recharge comes from the area between RW-13 and RW-25 (Fig. 7a and SM 4), which represents 34–64% of the total annual subsurface recharge from the mountain block to the alluvial aquifers from 1982 to 2009. The estimated subsurface recharge obtained from the SEAWAT model correlates with flooding during different time periods as reported by Himida (1997), JICA (1999) and Cools et al. (2012), as well as the historical records of water level and salinity. The model is valid for most regions included in the model, except for the areas close to the coast and within the sabkha deposits. The poor fit in the sabkha deposit area is because the model does not explicitly simulate rock-water interactions. In the coastal region, the model performs poorly due to areas of large horizontal concentration gradients due to seawater intrusion. This can be attributed to the relatively large grid resolution (100 m) and imprecise well locations close to the coast.

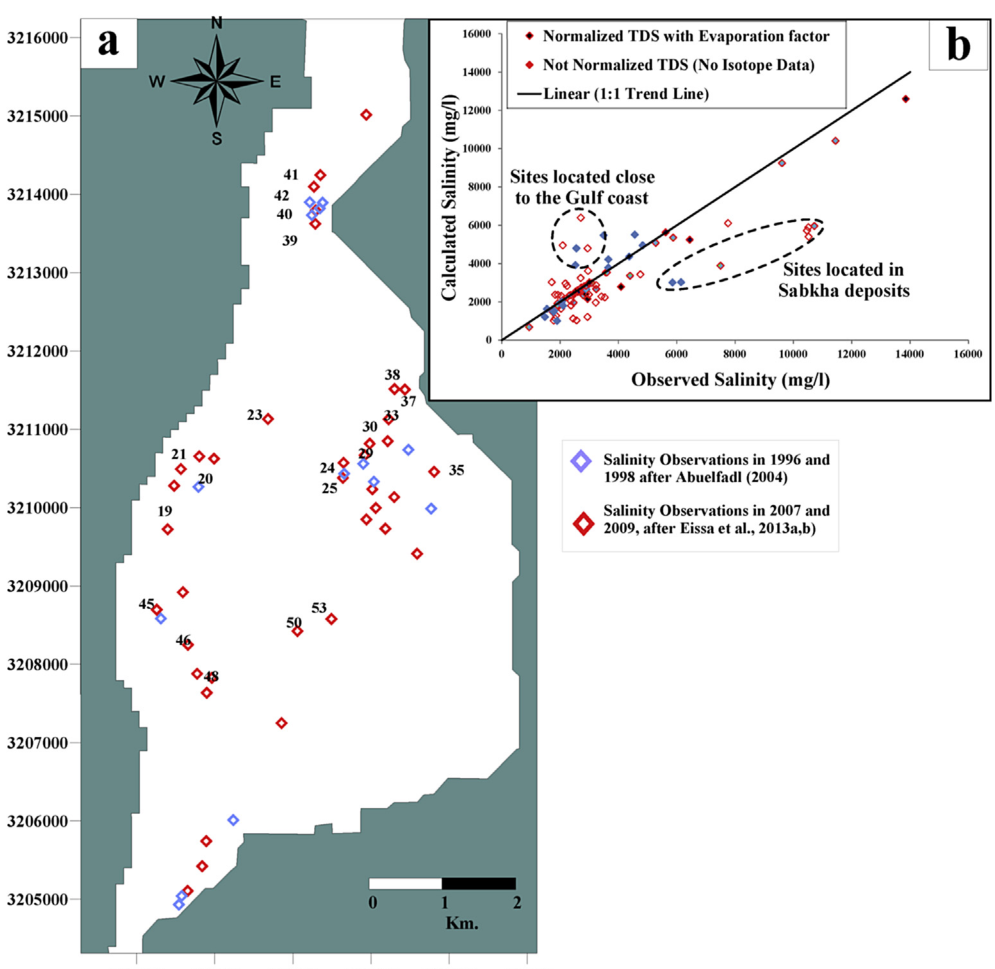

Fig. 9. a) Well location map for salinity observations. b) Calculated versus observed groundwater salinity. The model is valid for the majority of model domains except for the area close to the coast and the area located near sabkha deposits. Increased salinity from evaporation was calculated for samples with stable isotopic data (shown as "normalized TDS with evaporation factor" samples on the plot). The data are presented in SM 3.

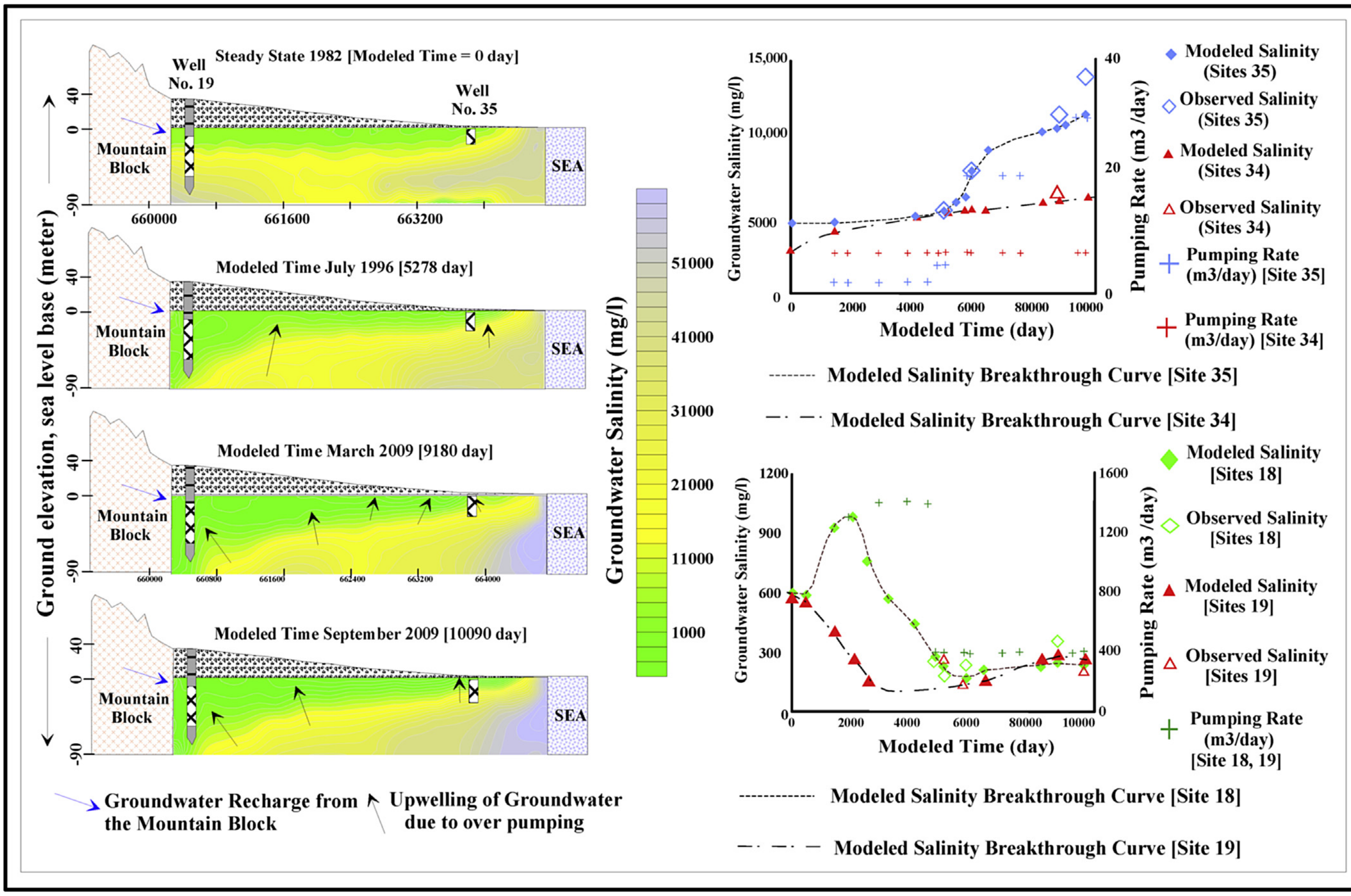

Fig. 10. Modeled groundwater salinity for different time periods and salinity breakthrough curves for different wells tapping Quaternary alluvial aquifers in the Wadi Watir delta. Well locations are shown on Fig. 1.

5. Conclusions

Groundwater chemistry in the Wadi Watir delta alluvial aquifers evolves from a low salinity Na:SO_4 water type to a more saline Mg:Cl water type by mineral and salt dissolution, cation exchange, and shallow groundwater evaporation. Groundwater in deeper wells in the main well field, and some wells along the coast have evolved into a Ca:Cl water type. This evolution is largely due to the upwelling of deep saline water, of marine origin, beneath the main well field caused by overpumping and seawater intrusion along the coast. Sulin's diagram supports that these processes, and the mixing of different water sources, produce the observed changes in water chemistry in the alluvial aquifers.

Groundwater in the main well field has low $^{87}Sr/^{86}Sr$ and $\delta^{81}Br$ values and high $\delta^{37}Cl$ values, indicating that deep saline groundwater is mixing with the main well field groundwater. The low $\delta^{81}Br$ values and high $\delta^{37}Cl$ values are attributable to their origins from old marine deposits. The $\delta^{37}Cl$ and $^{87}Sr/^{86}Sr$ isotope values have been used in the solute-weighted mass balance models to estimate the mixing ratios from different end member groundwaters. Groundwater in the main well field contains 4–10% of a deep saline groundwater and there is no evidence of mixing with modern seawater. Salinization of some shallow groundwaters located along the coast is from seawater intrusion (2–6%) and mixing with a deep saline groundwater (18–29%).

A groundwater flow and solute transport model was calibrated using observed and modeled salinity and water level data. The total average pumping rate for all wells in the main well field, from 1982 to 2009, was estimated to be 3100 m^3/day. In comparison, the total average pumping rate for all hand-dug wells in the Wadi Watir delta is 60 m^3/day. The model calculated average annual recharge is 2.16×10^6 m^3/year for the period 1982 to 2009, but it is highly variable because of the sporadic nature and intensity of precipitation events. Calibrating a groundwater flow and solute transport model using both water level and salinity data provides a better estimate of average annual recharge than using water level data alone.

There are five primary sources of salinity that affect water chemistry in the Wadi Watir delta alluvial aquifers: (1) dissolution of minerals and salts from the aquifer matrix, (2) upwelling of deep saline groundwater because of over pumping, (3) seawater intrusion along the coast, (4) leaching of salts from sabkha deposits near the coast, and (5) evaporation of shallow groundwater. The amount of upwelling saline groundwater could be reduced by decreasing pumping rates and/or adjusting well screen intervals to be shallower in newly drilled wells. In the Wadi Watir delta, groundwater outside of the main well field and sabkha areas is characterized by relatively low salinity compared with the other groundwaters in the delta area. Therefore, constructing more shallow wells in this area may provide more potable water. However, even groundwater in this area cannot be extensively developed on a sustainable basis because of the low rate of average annual recharge to the Wadi Watir delta alluvial aquifers.

Acknowledgements

Acknowledgement goes to the Egyptian Cultural and Educational Bureau in Washington DC, USA and in Montreal, Canada; the

Desert Research Center in Egypt; the Desert Research Institute George Burke Maxey Fellowship; the IT2 Isotope Tracers and Technologies, Inc., in Waterloo, Canada; and the Desert Research Institute in Reno, Nevada for funding this research and providing logistical and technical support. Many thanks and appreciation goes to Amy Hennessy for editing and improving the language of the manuscript, as a native speaker.

Appendix A. Supplementary data

Supplementary data related to this article can be found at http://dx.doi.org/10.1016/j.apgeochem.2016.05.017.

References

Abbas, A.M., Atya, A.A., Al-Sayed, E.A., Kamei, H., 2004. Assessment of groundwater resources of the Nuweiba area at Sinai Peninsula, Egypt by using geoelectric data corrected for the influence of near surface in homogeneities. J. Appl. Geophys. 56 (2), 107–122.

Abd El Hafez, A.A., 2001. Chemical Evaluation and Possible Treatment Sea Water Intrusion in the Groundwater in Some Coastal Areas, South Sinai. M. Sc. Thesis. Fac. Sci., Al Azhar Univ.

Abuelfadl, M.M., 2004. Geochemistry of Groundwater in Coastal Areas, South Sinai, Egypt. Ph.D. Thesis. Fac. Sci., Ain Shams Univ., Egypt.

Alsharhan, A.S., Rizk, Z.A., Nairn, A.E.M., Bakhit, D.W., Alhajari, S.A., 2001. Hydrogeology of an Arid Region: the Arabian Gulf and Adjoining Areas. Elsevier, The Netherlands.

Arth, J.G., Hanson, G.N., 1975. Geochemistry and origin of early Precambrian crust of the northeast Minnesota. Geochim. Cosmochim. Acta 39, 325–362.

Bartov, Y., Steinitz, G., Eyal, M., Eyal, Y., 1979a. The development of the Arava Rift Valley and the Red sea. New evidence for Cenozoic strike slip faults in eastern Sinai. In: Abstracts, Annual Meeting of Sede Boqer. Israel Geol. Soc, p. 8.

Bartov, Y., Steinitz, G., Eyal, M., Eyal, Y., 1979b. Horizontal groundwater flow systems in southern Sinai 325 displacement along faults, Bir Zreir eastern Sinai. In: Abstract, Annual Meeting at Sede Boqer. Israel Geol. Soc, p. 10.

Baxter, G.P., Wallace, C.C., 1916. Changes in volume upon solution in water of halogen salts of alkali metals, II. J. Am. Chem. Soc. 38 (1), 70–104.

Bielski, M., 1982. Stages in the Evolution of Arabian-nubian Massif in Sinai. Ph.D. Thesis. Hebrew Univ., Jerusalem, 155 pp.

Clark, I., 2015. Groundwater Geochemistry and Isotopes. CRC Press, Boca Raton, Florida.

Clark, I., Fritz, P., 1997. Environmental Isotopes in Hydrogeology. Lewis, New York.

Collins, A., 1975. Geochemistry of Oli-field Waters. Elsevier, New York.

Cools, J., Vanderkimpen, P., El Afandi, G., Abdelkhalek, A., Fockedey, S., El Sammany, M., Abdallah, G., El Bihery, M., Bauwens, W., Huygens, M., 2012. An early warning system for flash floods in hyper-arid Egypt. Nat. Hazards Earth Syst. Sci. 12, 443–457.

Du, Y., Ma, Y., Chen, L., Shan, H., Xiao, C., Lu, Y., Liu, C., Cai, H., 2015. Genesis of salinized groundwater in Quaternary aquifer system of coastal plain, Laizhou Bay, China: geochemical evidences, especially from bromine stable isotope. Appl. Geochem 59, 155–165.

Eastoe, C.J., Peryt, T.M., Petrychenko, O.Y., Cussey, G., 2007. Stable chlorine isotopes in Phanerozoic evaporites. Appl. Geochem 22, 575–588.

Eggenkamp, H.G.M., 1994. The Geochemistry of Chlorine Isotopes. Doctoral thesis. Faculteit Aardwetenschappen, Universiteit Utrecht, Netherlands.

Eggenkamp, H.G.M., Coleman, M.L., 2000. Rediscovery of classical methods and their application to the measurement of stable bromine isotopes in natural samples. Chem. Geol. 167 (3–4), 393–402.

Eggenkamp, H.G.M., Kreulen, R., Koster van Groos, A.F., 1995. Chlorine stable isotope fractionation in evaporites Geochem. Cosmochim. Acta 59, 5169–5175.

Eissa, M., 2012. Groundwater Resource Sustainability in Wadi Watir Watershed, Sinai, Egypt. Dissertation, submitted in partial fulfillment of the requirements for the degree of Doctor of Philosophy in Hydrogeology University of Nevada, Reno, August, 2012 UMI Number: 3539186.

Eissa, M., Parker, B., Shouakar-Stash, O., Hosni, M.H., El Shiekh, A., 2015b. Electrical resistivity tomography, geochemistry and isotope tracers for salt water intrusion characterization along the Northwestern coast. Egypt. Geol. Soc. Amer. Abstr. Progr. 47 (7), 486.

Eissa, M., Shouakar-Stash, O., Parker, B., De Dreuzy, J., 2015a. Managing saltwater intrusion in a poorly-constrained arid aquifer, utilizing isotopes and geochemistry, Northwestern coast. Egypt. Geol. Soc. Amer. Abstr. Progr. 47 (7), 324.

Eissa, M., Thomas, J.M., Dawoud, M., Pohll, G.M., Gomaa, M.A., Dahab, K.A., Hershey, R.L., 2010. Groundwater resource sustainability in Wadi Watir, gulf of Aqaba, Sinai, Egypt. In: Tenth Inter. Conf. On Development of Drylands, Meeting the Challenge of Sustainable Development in Drylands under Changing Climate – Moving from Global to Local, Session, p. 61.

Eissa, M., Thomas, J.M., Hershey, R.L., Pohll, G.M., Dawoud, M.I., Dahab, K.A., Gomaa, M.A., Shabana, A.R., 2013a. Geochemical and isotopic evolution of groundwater in the Wadi Watir watershed, Sinai Peninsula. Egypt. Environ. Earth Sci. 71 (4), 1855–1869.

Eissa, M., Thomas, J.M., Pohll, G.M., Hershey, R.L., Dahab, K.A., Dawoud, M.I., Gomaa, M.A., El Shiekh, A., 2013b. Groundwater resource sustainability in the Wadi Watir delta, gulf of Aqaba. Hydrogeol. J. 21 (8), 1833–1851.

El Ghazawi, M.M., 1999. Reconsideration of hydrogeologic setting in the delta of Wadi Watir, southern Sinai. Bull. Sci. 26 (1). Mansoura Univ., Egypt.

El Kiki, M.F., Eweida, E.A., El-Refeai, A.A., 1992. Hydrogeology of the Aqaba rift border province. In: Proc. 3rd Conf. Geol. Sinai Develop, Ismailia, Egypt, pp. 91–100.

El-Refaei, A.A., 1992. Water Resources of Southern Sinai, Egypt Geomorphological and Hydrogeological Studies. Ph.D. Thesis. Fac. Sci., Cairo Univ., Egypt.

El Sayed, M.H., 2006. Comparative study of water quality of the Quaternary aquifer in Wadi Watir basin and its delta, Southeast Sinai, Egypt. Egypt. J. Desert Res. 56 (1), 17–46.

El-Shazly, E.M., Abddel-Hady, M.A., El-Ghawaby, M.A., El-Kassas, I.A., El-Shazly, M.M., 1974. Geology of Sinai Peninsula from ERTS-1 Satellite Images. Remote Sensing Research Project, Academy of Scientific Research and Technology, Cairo, Egypt, p. 20.

Eyal, Y., 1973. The tectonics of the Shelomo and Yotam Grabens, Eilat, Israel. Isr. J. Earth Sci. 22, 165–184.

Eyal, M., Bartov, Y., Shimron, A.E., Bentor, Y.K., 1980. Sinai Geologic Map, Scale 1: 500,000. Ministry of Energy and Infrastructure, Admin. For Res. in Earth Sci., Israel.

Faure, G., 1986. Principles of Isotope Geology, second ed. Wiley, New York.

Fetter, C.W., 2001. Applied Hydrogeology. Merrill Publishing, Columbus, OH.

Fishman, M.J., Friedman, L.C., 1985. Methods for determination of inorganic substances in water and fluvial sediments. In: U.S. Geol. Surv. Book, 5. Chapter A1, Open File Report 85–495, Denver, Colorado, U.S.A.

Frape, S.K., Blyth, A., Blomqvist, R., McNutt, R.H., Gascoyne, M., 2004. Deep fluids in the continents: II. Crystalline rocks. In: Drever, J.I. (Ed.), Surface and Ground Water, Weathering, and Soils. Treatise on Geochemistry, 5. Elsevier, New York, 541–540.

Gavish, E., 1974. Geochemistry and mineralogy of a recent sabkha along the coast of Sinai, Gulf of Suez. Sedimentology 21, 397–414.

Gelhar, L.W., Welty, C., Rehfeldt, K.W., 1992. A critical review of data on field-scale dispersion in aquifers. Water Resour. Res. 28 (7), 1955–1974.

Gonfiantini, R., 1986. Environmental isotopes in lake studies. In: Fritz, P., Vents', Ch (Eds.), Handbook of Environmental Isotopes Geochemistry, vol. 2. The Terrestrial Environment., B. Elsevier, Amsterdam, The Netherlands, pp. 112–168.

Guo, W., Langevin, C.D., 2002. User's Guide to SEAWAT: a Computer Program for Simulation of Three-dimensional Variable-density Ground-water Flow: Techniques of Water-resour. Invest. Book 6, Chapter A7 (Supersedes OFR 01–434).

Harbaugh, A.W., Banta, E.R., Hill, M.C., McDonald, M.G., 2000. MODFLOW- 2000, the U.S. Geological Survey Modular Ground-water Model – User Guide to Modularization Concepts and the Ground-water Flow Processes, U.S. Geol. Sur. Open-file Report.

Himida, I.H., 1997. Water Resources of Wadi Watir. Internal Report. Desert Research Center (in Arabic).

IAEA, 1993. Mathematical models and their applications to isotope studies in groundwater hydrology. In: Proceedings of a Final Research Co-ordination Meeting Held in Vienna, 1–4 June 1993.

Isawi, H., El-Sayed, M.H., Eissa, M., Shouakar-Stash, O., Shawky, H., Abdel Mottaleb, M.S., 2016. Integrated geochemistry, isotopes, and geostatistical techniques to investigate groundwater sources and salinization origin in the Sharm EL-Shiekh Area, South Sinia, Egypt. Water Air Soil Pollut. 227, 151.

Ismail, Y.L., 1998. Hydrogeological and Hydrochemical Studies on Wadi Watir Area, South Sinai, Egypt. PhD Thesis. Fac Sci, Suez Canal Univ, Egypt.

Issar, A., Gilad, D., 1982. Groundwater flow systems in the arid crystalline province of Southern Sinai. Hydrol. Sci. J. des Sci. Hydrol. 27, 3–9.

Japan International Cooperation Agency (JICA) and Water Resources Research Institute (WRRI), 1999. South Sinai Groundwater Resources Study in the Arab Republic of Egypt. Main Report. Pacific Consultants International, Tokyo.

Kaufmann, R., Long, A., Bentley, H., Davis, S., 1984. Natural chloride isotope variations. Nature 309, 338–340.

Khalil, H.M., 2010. Hydro-geophysical configuration for the quaternary aquifer of Nuweiba Alluvial fan. J. Environ. Eng. Geophys. 15 (2), 77–90.

Kirk, S.T., Campana, M.E., 1990. Deuterium-calibrated groundwater flow model of a regional carbonate-alluvial system. J. Hydrol. 119, 357–388.

Langevin, C.D., Guo, W., 2006. MODFLOW/MT3DMS-based simulation of variable density ground water flow and transport. Groundwater 44 (3), 339–351.

Liebscher, A., Lüders, V., Heinrich, W., Schettler, G.G., 2006a. Br/Cl signature of hydrothermal fluids: liquid–vapour fractionation of bromine revisited. Geofluids 6, 113–121.

Liebscher, A., Barnes, J., Sharp, Z., 2006b. Chlorine isotope vapor–liquid fractionation during experimental fluid-phase separation at 400 °C/23 MPa to 450 °C/42 MPa. Chem. Geol. 234, 340–345.

Liu, Y., Yamanaka, T., Zhou, X., Tian, F., Mab, W., 2014. Combined use of tracer approach and numerical simulation to estimate groundwater recharge in an alluvial aquifer system: a case study of Nasunogahara area, central Japan. J. Hydrol. 519, 833–847.

Lyons, W.B., Tyler, S.W., Gaudette, H.E., Long, D.T., 1995. The use of strontium isotopes in determining groundwater mixing and brine fingering in a playa spring zone, Lake Tyrrell, Australia. J. Hydrol. 167 (1–4), 225–239.

Mabrouk, M.A., Nasr, I.M., 1997. The hydrogeologic setting in the delta of Wadi Watir, Gulf of Aqaba, a geoelectrical resistivity sounding approach. Desert Inst.

Bull. Egypt 47 (1), 149–162.
Malosazewski, P., Rauert, W., Stichler, W., Herrmann, A., 1989. Application of flow models in an Alpine catchment area using tritium and deuterium data. J. Hydrol. 66, 319–330.
McNutt, R.H., Frape, S.K., Fritz, P., 1984. Strontium isotopic composition of some brines from the precambrian shield of Canada. Chem. Geol. Isot. Geosci. 2, 205–215.
McNutt, R.H., Frape, S.K., Fritz, P., Jones, M.G., MacDonald, I.M., 1990. The $^{87}Sr/^{86}Sr$ values of Canadian shield brines and fracture minerals with applications to groundwater mixing, fracture history, and geochronology. Geochim. Cosmochim. Acta 54, 202–215.
Negrel, P.H., Casanova, J., Kolppman, W., Aranyossy, J.F., 2002. A combined isotopic tool box for the investigation of water-rock interaction: an overview of Sr, B, O, H isotopes and U-series in deep groundwaters from the Vienne granitoid (France). Water Rock Interact. 40, 1–38.
Plumacher, J., Kinzelbach, W., 2000. Calibration of a regional groundwater flow model using environmental isotope data. In: Tracers and Modelling in Hydrogeology (Proceedings of the TraM'2000 Conference Held at Liège, Belgium May 2000). IAHS Publ. No. 262.
Rainwater, F.H., Thatcher, L.I., 1960. Methods for collection and analysis of water samples. U.S. Geol. Surv. Water Supply Paper 1454.
Said, R., 1962. The Geology of Egypt. Elsevier, Amsterdam.
Salma, F., Bouhlila, R., Tarhouni, J., 2010. Hydrochemical processes at the seawater/freshwater interface as indicators of seawater intrusion evolution: case of Korba coastal plain (Tunisia). In: SWIM21–21st Salt Water Intrusion Meeting.
Schoeller, H., 1962. Les Eaux Souterrains. Masson & Cie, Paris.
Sefelnasr, A., Sherif, M., 2014. Impacts of seawater rise on seawater intrusion in the nile delta aquifer, Egypt. Groundwater 52, 264–276.
Shalaby, A.I., 1997. Geomorphology and Hydrogeology of Wadi Watir Basin, S. E. Sinai, Egypt. M.Sc. Thesis. Fac. Sci., Mansoura Univ., Egypt.
Shmulovich, K.I., Landwehr, D., Simon, K., Heinrich, W., 1999. Stable isotope fractionation between liquid and vapour in water-salt systems up to 600°C. Chem. Geol. 157, 343–354.
Shouakar-Stash, O., 2008. Evaluation of Stable Chlorine and Bromine Isotopes in Sedimentary Formation Fluids. University of Waterloo. Ph.D. thesis.
Shouakar-Stash, O., Alexeev, S.V., Frape, S.K., Alexeeva, L.P., Drimmie, R.J., 2007. Geochemistry and stable isotope signatures, including chlorine and bromine isotopes, of the deep groundwaters of the Siberian Platform, Russia. Appl. Geochem 22 (3), 589–605.
Shouakar-Stash, O., Drimmie, R.J., Frape, S.K., 2005a. Determination of inorganic chlorine stable isotopes by continuous flow isotope ratio mass spectrometry. Rapid Commun. Mass Spectrom. 19, 121–127.
Shouakar-Stash, O., Frape, S.K., Drimmie, R.J., 2005b. Determination of bromine stable isotopes using continuous-flow isotope ratio mass spectrometry. Anal. Chem. 77, 4027–4033.
Sibanda, T., Nonner, J.C., Uhlenbrook, S., 2009. Comparison of groundwater recharge estimation methods for the semi-arid Nyamandhlovu area, Zimbabwe. Hydrogeol. J. 17, 1427–1441.
Stober, I., Bucher, K., 2002. Water-rock Interaction. Kluwer Academic Publishers, London.
Stotler, R.L., Frape, S.K., Shouakar-Stash, O., 2010. An isotopic survey of $\delta^{81}Br$ and $\delta^{37}Cl$ of dissolved halides in the Canadian and Fennoscandian Shields. Chem. Geol. 274 (1–2), 38–55.
Sulin, V.A., 1946. Vody Neftyanykh Mestorozhdenii v Sisteme Prirodnikh Vod Gostoptekhizdat, Moscow.
United States Geological Survey (USGS), 2004. Reprocessing by the Global Land Cover Facility, 2004, (30) Arc Second SRTM Elevation. The GLCF, College Park, Maryland. http://www.landcover.org.
Vengoush, A., 2014. Salinization and saline environments. Environmental geochemistry, vol. 9, Sherwood Lollar, B. (ed.), Treatise in Geochemistry Second Edition. 11, 325–378.
Weyhenmeyer, C.E., 2002. Groundwater evolution in an Arid Coastal Region of the sultanate of Oman based on geochemical and isotopic tracers. In: Water-rock Interaction, 40. Springer, Netherland, pp. 1–38.
Zheng, C., Bennett, G.D., 1995. Applied Contaminant Transport Modeling, Theory and Practice. Wiley, New York.
Zheng, C., Wang, P.P., 1999. MT3DMS Documentation and User's Guide. Contract Report SERDP-99–1. U.S. Army Engineer Research and Development Center, Vicksburg, MS.